

# Structure of the Colcemid-Treated PtK<sub>1</sub> Kinetochore Outer Plate as Determined by High Voltage Electron Microscopic Tomography

Bruce F. McEwen,\* James T. Arena,\* Joachim Frank,\*\* and Conly L. Rieder\*\*

\*Wadsworth Center for Labs and Research, Empire State Plaza, Albany, New York 12201-0509; and †Department of Biomedical Sciences, State University of New York, Albany, New York 12222

**Abstract.** High voltage electron microscopic tomography was used to determine the organization of the kinetochore plate and its attachment to the underlying chromosome. Six reconstructions were computed from thick sections of Colcemid-treated PtK<sub>1</sub> cells and analyzed by a number of computer graphics methods including extensive thin slicing, three-dimensional masking, and volume rendering. When viewed en-face the kinetochore plate appeared to be constructed from a scaffold of numerous 10–20-nm thick fibers or rods. Although the fibers exhibited regions of parallel alignment and hints of a lattice, they were highly variable in length, orientation and spacing. When viewed in stereo, groups of these fibers were often seen oriented in different directions at different depths to give an overall matted appearance to the structure. When viewed “on edge,” the plate was 35–40 nm thick, and in thin slices many regions were tripartite with electron-opaque domains, separated by a more translucent middle layer, forming the inner and outer plate boundaries. These domains were joined at irregular intervals. In some slices, each domain appeared as a linear array of 10–20-nm dots or rods embedded in a less

electron-opaque matrix, and adjacent dots within or between domains often appeared fused to form larger blocks. The plate was connected to the underlying chromosome by less densely arrayed 10–20-nm thick fibers that contacted the chromosome-facing (i.e., inner) surface of the plate in numerous patches. These patches tended to be arrayed in parallel rows perpendicular to the long axis of the chromosome. In contrast to connecting fibers, corona fibers were more uniformly distributed over the cytoplasmic-facing (i.e., outer) surface of the plate. When large portions of the reconstructions were viewed, either en-face or in successive slices parallel to the long axis of the chromosome, the edges of the plate appeared splayed into multiple “fingers” that partly encircled the primary constriction. Together these observations reveal that regions of the kinetochore outer plate contain separate structural domains, which we hypothesize to serve separate functional roles. Our three-dimensional images of the kinetochore are largely consistent with the hypothesis that the outer plate is composed of multiple identical subunits (Zinkowski, R. P., J. Meyne, and B. R. Brinkley. 1991. *J. Cell Biol.* 113:1091–1110).

**I**N the past, the kinetochore was viewed simply as the chromosomal attachment site for spindle microtubules (MTs)<sup>1</sup> during cell division (reviewed in Schrader, 1953; Rieder, 1982; Brinkley et al., 1989). However, recent evidence reveals that the kinetochore is a functionally complex organelle that produces the force for poleward chromosome motion (Gorbsky et al., 1987; Nicklas, 1989; Rieder and Alexander, 1990), while simultaneously holding its associated MT ends as they grow and shorten by subunit addition/deletion within its confines (Mitchison et al., 1986; Mitchison, 1988; Wise et al., 1991). In view of this new evidence, a thorough understanding of kinetochore structure becomes important in elucidating the mechanism(s) by which this complex biological machine functions.

1. *Abbreviations used in this paper:* HVEM, high voltage electron microscopic; MT, spindle microtubule.

Kinetochore morphogenesis has been best described for mammalian cells (especially PtK: reviewed in Roos, 1973; Rieder, 1982). During prophase, the kinetochore is a finely-fibrillar ball of material closely associated with the more electron dense heterochromatin of the forming primary constriction. After nuclear envelope breakdown, but before the acquisition of MTs, this ball differentiates into a disk- or plate-shaped structure that is attached to the underlying chromosome by a less opaque region traversed by thin fibers. In some preparations, that part of the chromosome subadjacent to the plate is more electron dense than the remainder of the chromosome. A moderately dense fibrillar “corona” radiates a variable distance from the cytoplasmic face of the plate. The plate diameter varies between species, but with few exceptions (e.g., Brinkley et al., 1984) it is similar between the chromosomes of a genome regardless of their size

(usually 0.5–1.0  $\mu\text{m}$  diam). Kinetochores of untreated cells, which have not yet associated with spindle MTs, resemble those found in Colcemid-treated mitotic cells in which spindle assembly is inhibited (e.g., Rieder, 1982).

Despite its central role in chromosome distribution, very little is known with certainty regarding the three-dimensional structure of the vertebrate kinetochore. Structural and compositional studies are complicated by its diminutive size and complex fibrillar construction which resembles that of the underlying chromatin (e.g., Earnshaw and Tomkiel, 1992). The former makes the electron microscope the only available tool for studying kinetochore structure, while the latter necessitates the development of novel approaches for differentiating subtle structural differences in three dimensions. Indeed, the outer kinetochore plate has been examined in whole mounts of isolated chromosomes before (e.g., Moses and Counce, 1974) or after selective digestions (Rattner, 1986), within serial-thin sections after various treatments (e.g., Brinkley and Stubblefield, 1970; Roos, 1977; Brinkley et al., 1980), by stereo imaging of thick sections after various treatments (e.g., Ris and Witt, 1981), and by SEM (Rattner, 1987). These efforts have produced a number of conflicting models regarding the structural organization of the kinetochore plate (e.g., Roos, 1977; Ris and Witt, 1981; Rattner, 1986).

Most recently Zinkowski et al. (1991) proposed that the kinetochore plate is constructed from repetitive MT-binding sites. These sites are envisioned to be composed of unique proteins and repeat satellite DNA sequences that arise from the heterochromatin of the primary constriction (Masumoto et al., 1989; Cooke et al., 1990). Multiple units are envisioned to run the full width of the plate and be aligned in parallel register, perpendicular to the long axis of the chromosome. Although the model of Zinkowski et al. (1991) provides a straightforward mechanism for kinetochore evolution, its critical component concerns the structural organization of the outer plate which remains controversial.

Electron microscopic tomography, particularly when combined with high voltage EM, is emerging as an effective method for analyzing the three-dimensional ultrastructure of cellular components (Frank, 1992; McEwen, 1992; Woodcock, 1992). For this approach, many different views of the structure are collected by tilting a thick section of the specimen within the electron microscope. After appropriate alignment and density normalization, the tilt series is used to compute a three-dimensional reconstruction according to well-established mathematical principles (Crowther et al., 1970; Gilbert, 1972; Frank and Radermacher, 1986). The resulting reconstruction is a point-by-point three-dimensional density map of the structure, which can then be viewed from any angle and analyzed with a number of computer graphic tools.

In this study we present the three-dimensional ultrastructure of large segments of the kinetochore plate found in thick sections of mitotic mammalian cells depleted of spindle MTs by Colcemid treatment. These high-voltage electron microscopic (HVEM) tomographic reconstructions clearly demonstrate that the structure of the outer kinetochore plate is more complex than previously envisioned, and provide unique information regarding how this plate is attached to the underlying chromosome.

## Materials and Methods

### Cell Culture and Specimen Preparation

Actively growing PtK<sub>1</sub> cells were incubated overnight in 1.0  $\mu\text{M}$  Colcemid before fixation in 37°C glutaraldehyde (2% in 0.1 M PO<sub>4</sub> buffer, pH 6.9) for 30 min. After this initial fixation the cultures were postfixated at 4°C in OsO<sub>4</sub> (1% in buffer) for 15 min, dehydrated in a graded series of ethanols, and flat embedded in Epon-Araldite (e.g., see Jensen et al., 1987). Selected mitotic cells were excised from the embedments, mounted on plastic pegs, and cut into serial 0.20–0.25- $\mu\text{m}$  thick sections. The ribbons of sections were mounted in the middle of 1  $\times$  2 mm Formvar-coated slot grids, and stained in uranyl acetate and lead citrate as described by Rieder et al. (1985). After staining, each grid was briefly placed on a drop of diluted colloidal gold (15 nm) suspension in order to introduce fiducial markers.

### Electron Microscopy and Three-Dimensional Reconstruction

Three different tilt series of HVEM micrographs were recorded at 1.0 MV from sections containing kinetochores cut either parallel or perpendicular to the chromosomal long axis. All series were recorded at an initial magnification of 20,000 using the high-precision tilt stage designed for the Albany HVEM (Turner et al., 1988). Two of these series were recorded on adjacent serial sections and in each series the angular increment was 2° with a minimum range of  $\pm 60^\circ$ . Six of the kinetochore segments contained within these three tilt series were processed for tomography. All micrographs were digitized using an Eikonix EC 78/99 digital camera (Ektron Corp., Bedford, MA) with a pixel size of 3.5 nm.

The digitized images were rotationally aligned with the aid of gold fiducial markers, using a least-squares based computer algorithm developed by Lawrence (Luther et al., 1988; Lawrence, 1992), so that the tilt axis corresponded to the *y* (vertical) axis. Density normalization, translational alignment and weighted back-projection reconstruction were conducted as previously described by McEwen et al. (1986) and Frank et al. (1987).

### Reconstruction Analyses

As detailed in McEwen et al. (1986) all of the three-dimensional reconstructions were low-pass filtered to their limiting resolution of 12 nm as determined by the criterion of Crowther et al. (1970) and Radermacher's (1992) modification for objects that are much wider in the *x-y* plane than in section thickness. The computed reconstructions were then examined as single slices and volume renderings. The latter were created on either a PIXAR or Silicon Graphics IRIS VGX 4D/340 computer graphics workstation. Those computed on the PIXAR workstation used this company's own software while the renderings on the Silicon Graphics used (VoxelView Vital Images Inc., Fairfield, Iowa). All other operations used for computing and examining the reconstructions are contained in the SPIDER image processing software system developed by Frank et al. (1981), and in implementation at the Albany Biological Microscopy and Image Reconstruction Biotechnological Resource (Albany, NY). Careful consideration was given to density thresholds and other parameters used to create the representations (see Frank et al., 1987; McEwen, 1992). The thresholds utilized in this study were chosen to simplify viewing the volume. In regard to this, it is important to stress that the major conclusions of this study were verified over a wide range of thresholds.

For interactive three-dimensional masking operations (McEwen et al., 1992) a mouse was used to draw a line around the area of interest in each 3.5-nm thick slice of the three-dimensional reconstruction. For the present study this included the kinetochore outer plate, connecting filaments and corona material. The specified component was then extracted from the slice through the creation of an intermediate mask file. The material within consecutive masks was then stacked to form a new version of the three-dimensional volume. Masked versions contained only the selected portion of the structure and could be rendered and viewed from any direction without interference from other components. Color-coded representations could be created by simultaneously placing different versions of the three-dimensional reconstructions into separate color channels of the monitor. A volume could even be double-masked by applying two sets of masked files. Under this condition only regions contained in both masks were represented, i.e., only points of overlap.

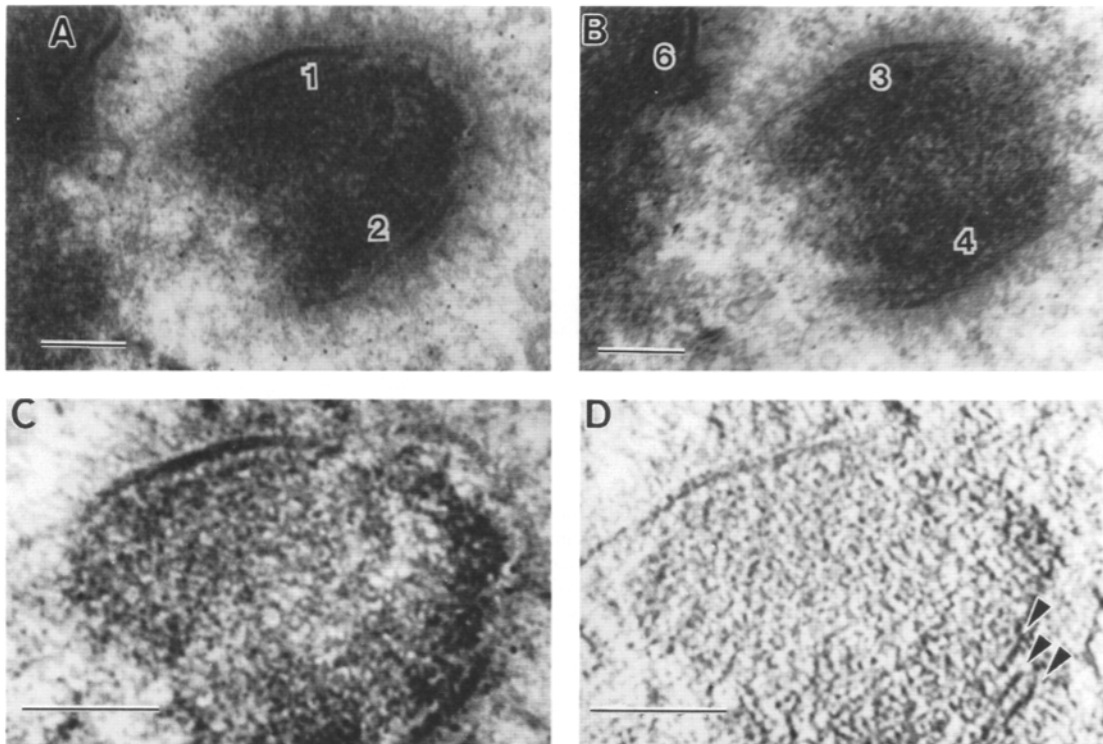


**Figure 1.** Selected views of the input tilt series and three-dimensional reconstructions of kinetochores from colcemid-treated PtK cells. (A) The untitled or 0° electron micrograph from the middle of three serial sections. Sister kinetochores are viewed from a direction parallel to the chromosomal long axis with the areas used for tomographic reconstructions 1 and 2 indicated. (B) The untitled view of a serial section sequential to (A) with the areas used for reconstructions 3, 4, and 6 indicated. Reconstruction 6 is from a neighboring chromosome and is viewed perpendicular to the chromosomal long axis. (C) A projection through the full volume of tomographic reconstruction 1. This view is equivalent to (A) and is obtained by “looking” through all 55 of the 3.5-nm slices that comprise the volume. (D) A 10.5-nm thick slice from reconstruction 1. This view was created by adding together three sequential 3.5-nm thick slices. Arrowheads indicate a region where the plate has splayed apart into three distinct segments. All bars, 0.25  $\mu\text{m}$ .

Because the operator must decide where the boundaries of the selected components lie in each individual slice, the masking procedure is inherently subjective. This was not a problem when isolating the outer plate, which had clearly-defined borders, or the corona, which was assumed to be all that material connected to and immediately distal to the cytoplasmic (outer) face of the plate. The fibers connecting the plate to the underlying chromatin were more problematic because it was not always clear whether material contacting the chromosomal (inner) face of the plate represented a significant connection to the chromosome. However, the major connections were readily identified and we are therefore confident that the results are a reasonable representation of the overall pattern.

## Results

For this study we generated six tomographic reconstructions from 0.20–0.25- $\mu\text{m}$  thick sections through four kinetochores. Three of these kinetochores are shown in the sequential sections pictured in Fig. 1, A and B. Two kinetochores (labeled 1 and 3, and 2 and 4 in Fig. 1, A and B) are sisters, cut perpendicular to the long axis of the chromosome, that are totally contained in, and followed through, three serial sections. The other two were reconstructed from single sections of separate kinetochores cut tangentially to the chromosomal long axis (e.g., 6 on Fig. 1 B). For the following discussion the numbers assigned to the kinetochore profiles in Fig. 1, A and B, are also used to identify the tomographic reconstruction of that profile. Because all of the reconstructions were

similar in major details, our results will be illustrated primarily from reconstructions 1, 2, and 5.

A projection of tomographic reconstruction 1, in the same direction as the untitled view in Fig. 1 A, is shown in Fig. 1 C. There are some minor differences in appearance because the reconstruction volume was low-pass filtered to the limiting resolution of 12 nm and some gold fiducial particles were removed. However, all of the essential features of the kinetochore and chromatin from the equivalent portion of Fig. 1 A are retained in the reconstruction. This type of comparison provides a test for some, but not all, possible errors in the reconstruction process. When combined with similar test views from other directions, all of the reconstructions were found to be accurate representations of the input data.

The analysis of a tomographic reconstruction, especially of a structure as intricate as the kinetochore-centromere complex, is not straightforward because all available media for viewing the reconstruction are two dimensional. A convenient way to begin the analysis is to decompose the reconstruction volume into a stack of planes, or two-dimensional slices, which are one voxel (3.5 nm) thick. Thicker slices, such as the 10.5-nm slice shown in Fig. 1 D, can be constructed by summing individual adjacent slices. Many features can be followed through the depth dimension by simply viewing the stack sequentially as represented in Fig. 2. For reconstructions 1, 2, 5 and 6, between 50–55 slices, 3.5-nm

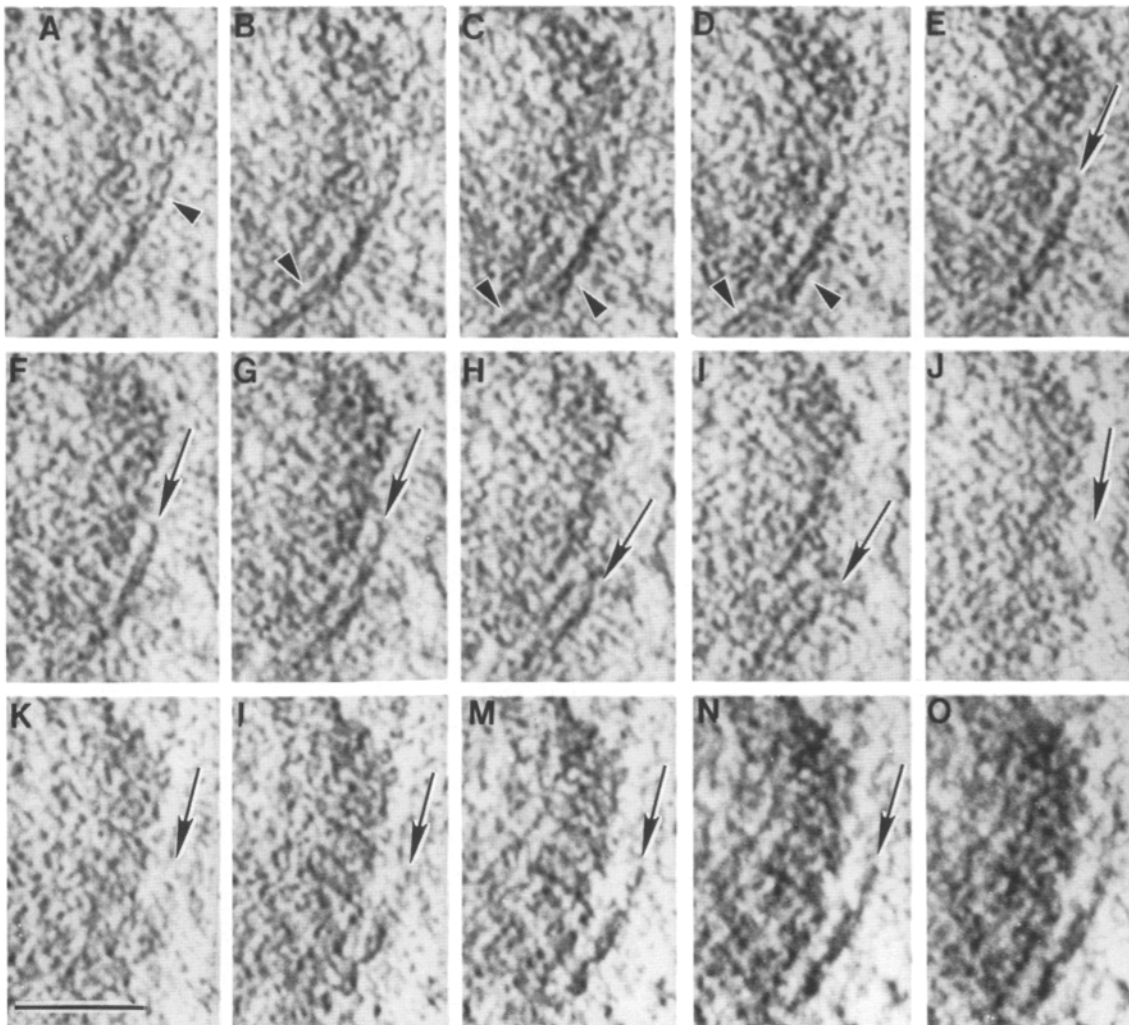


**Figure 2.** A gallery of successive 7.0-nm thick slices from a subvolume of reconstruction 1. The gallery traces through 105 nm of the full 185 nm depth of the reconstruction volume. Arrows denote plate fragmentation that is detected by following the structure through different frames, whereas arrowheads indicate areas in individual slices where the plate appears tripartite. Bar, 0.25  $\mu\text{m}$ .

thick, are required to fully represent that 185-nm thick part of the structure contained within the section.

Thin slices through a reconstruction provide detail not seen in projections through the whole structure (cf. Figs. 1, C and D, and 2). For example, the fibrous nature of the kinetochore plate and the underlying chromatin is much more evident in the thinner slices. The gallery of 7.0-nm thick slices presented in Fig. 2 reveals fragmentation in a portion, or

window, of kinetochore 2. Moreover, it is evident from these views that the peripheral edges of the kinetochore plate, when viewed parallel to the long axis of the chromosome, are splayed into 50–70-nm thick segments of irregular lengths (e.g., *arrowheads* in Fig. 1 D, *arrows* in Fig. 2). This feature, which was found in all of our reconstructions, is easily visualized in volume renderings of masked plates, where the periphery is seen splayed into multiple fingers which in

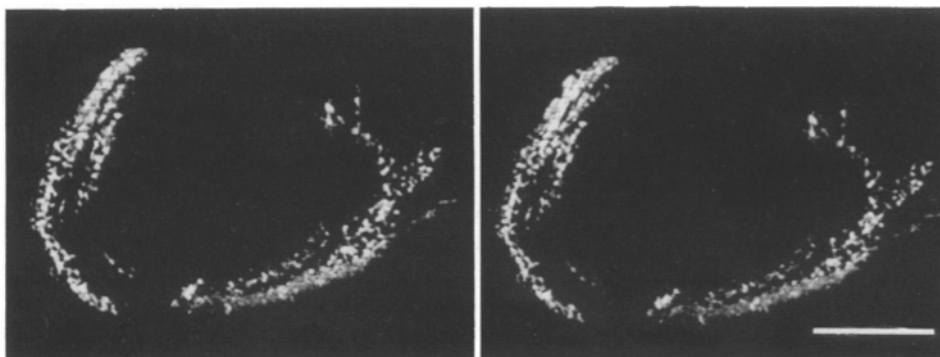


**Figure 3.** Stereo volume renderings of a masked version of reconstruction 1. The three-dimensional reconstruction was masked (see Materials and Methods) in order to isolate the plate structure for more effective viewing. The mass density of the plate appears with reverse contrast to that in Figs. 1 and 2 (i.e., white instead of black). Note splaying at the peripheral edges. Bar, 0.25  $\mu\text{m}$ .

this kinetochore wrap partly around the primary constriction (Fig. 3). Such a masking procedure was employed (see Materials and Methods) to form new versions of the reconstructions in which selected components could be viewed individually without interference from adjacent structures (e.g., Figs. 3 and 4).

The types of connections seen between the outer plate and the subjacent chromosome are illustrated in Fig. 5. The distribution of these 10–20-nm thick connections within reconstruction 1 is depicted by the color-coded three-dimensional volume renderings in Fig. 4 C, where the outer plate is orange, the connecting fibers green, and the overlap between the two yellow. Such renderings revealed that these connections occur both within the interior and at the periphery of the plate. The contact points between the connecting fibers and the inner surface of the outer plate could be depicted by double-masking the reconstructions as in Figs. 6, A and B. In all of the three reconstructions analyzed in this manner the connecting fibers were sparsely distributed over the inner surface of the outer plate to form punctate linear arrays that ran perpendicular to the long axis of the chromosome. A similar approach was used to view the distribution of corona fibers and the sites where they contact the outer plate surface (Figs. 4 D, 6 C). When compared with connecting fibers, the corona material is more extensive and distributed more randomly over the outer surface of the kinetochore plate.

The kinetochore outer plate is not rigid as evidenced by the fact that it is usually curved (e.g., Fig. 1), and sometimes even bent into acute angles (e.g., Fig. 7 A). When viewed en face it appears composed of regions of greater and lesser density which impart an overall matted appearance (Fig. 4, A and B). Upon closer inspection the plate can be seen to contain an extremely complex array of irregular fibrillar elements. These elements range in diameter from 20 to <10 nm, with the exact thickness being uncertain because of the 12-nm resolution limit of our reconstructions. In stereo en face views (Fig. 4, A and B), fibers in many regions of the plate are seen to be aligned into roughly parallel arrays which generally have a different orientation from fibers at other levels of the structure.

When viewed on edge, perpendicular or parallel to the long axis of the chromosome, the plate is 35–40-nm thick (Figs. 1, 2, 7, and 8). When examined through a full gallery of thin slices, the substructure of the plate varies considerably depending on the slice (e.g., Fig. 2) and, to a lesser extent, the viewing perspective relative to the chromosome long axis. However, all views observed appear to be different arrangements of a basic unit fiber that is 10–20 nm in diameter. In some slices these fibers tend to form clusters of linearly aligned 30–70-nm dense beads or blocks that were separated by smaller translucent regions (e.g., Fig. 7, C and D). This “block on a string” appearance is particularly evident when the plates are isolated by masking and then viewed on edge perpendicular to the chromosome long axis (*arrows* in Fig. 8). In other slices, the fibers appear separately as opaque dots or short rods that are embedded in a slightly less opaque matrix (Figs. 5 B, 7 A and B, and 8). The position of these elements with respect to one another is variable but in some sections they are aligned into rows that marked the top and bottom boundaries of the plate thickness (e.g., Figs. 7 A, 8, A–C). Finally, in portions of other slices, the plate

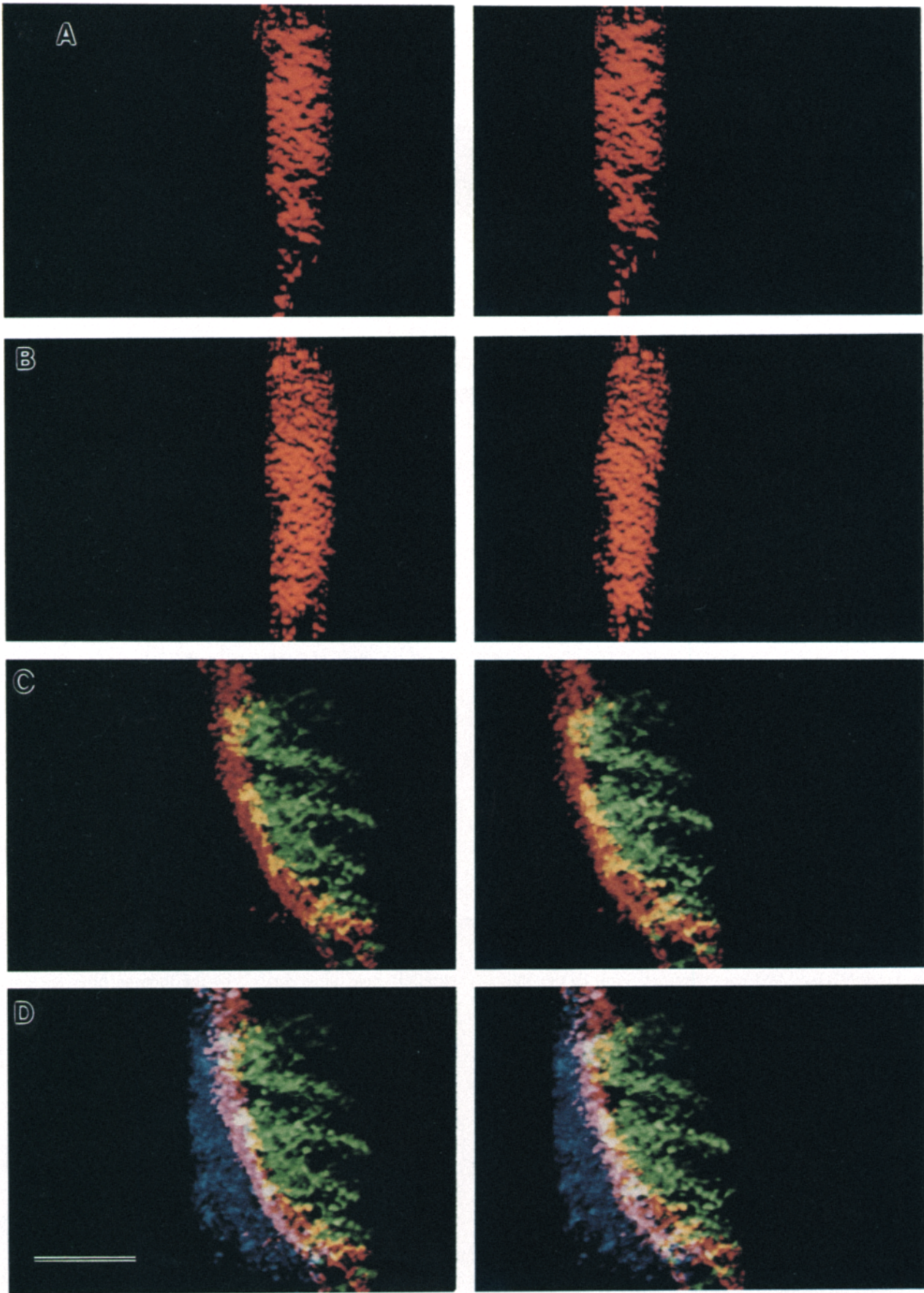
is seen to be structured as two largely continuous dense parallel fibrils, 10–20-nm thick, that are separated from each other by a more translucent region of similar or greater thickness (e.g., Fig. 2, 7, E and F). This tripartite composition is also evident when plates are isolated by masking, and then viewed on edge (*arrowheads* in Fig. 8 A–D).

A poorly defined inner plate, which is slightly more dense than the remainder of the chromatin, is sometimes seen associated with the chromosome surface beneath the outer plate. This structural feature is occasionally visible on the original electron micrographs (e.g., Fig. 1 B, kinetochore 4), but more clearly evident in some thin slices through the reconstructions (e.g., Figs. 5 A, 7, A and C). Because the focus of our work was on the outer plate and its associated structures, little emphasis is placed on detailing the structure of this feature.

## Discussion

With few exceptions the unattached (i.e., MT-free) kinetochore plate in vertebrates is considered to be 30–40-nm thick (Brinkley and Stubblefield, 1966; Krishan, 1968; Roos, 1973; Ris and Witt, 1981) and to be composed of numerous unique proteins (e.g., Comptom et al., 1991; Zinkowski et al., 1991; see however Earnshaw and Tomkiel, 1992) which are bound to an extensive fibrous scaffold. Most investigators consider the fibers comprising this structure to be 10–20-nm thick (Brinkley and Stubblefield, 1966; Krishan, 1968; Roos, 1973; Ris and Witt, 1981; see however Rattner, 1986), and to be arranged parallel within the plate as a single layer (e.g., Ris and Witt, 1981; Rattner, 1986; Zinkowski et al., 1991). Although our studies confirm that the primary structural scaffold of the outer plate is based on a 10–20-nm thick fiber, our electron microscopic tomographic reconstructions reveal that the organization of these fibers is considerably more complicated than previously modeled.

Our major findings regarding the three-dimensional structure of the kinetochore outer plate are interpreted schematically in Fig. 9. In summary, the outer plate is composed of 10–20-nm diam fibers, or rods, that are often roughly parallel. These elements are generally oriented in different directions on the two surfaces of the plate and this imparts an overall matted appearance to the structure (Figs. 4, A and B, 9). In regions where the fibers are closely associated, they appear fused into larger blocks while in regions where the fibers are more separated, the plate appears tripartite and even discontinuous (e.g., Figs. 2, A–D, 7 E and F, 8, A–C, 9). The tripartite regions effectively divide many areas of the plate into three separate structural domains: one that faces the chromosome, another that is destined to face the spindle pole, and a more electron translucent layer in between. Our conclusion that the outer plate is trilamellar is not without precedent. Many investigators have noted that the outer plate “consists of two bands approximately 150 Å wide, and joined at irregular intervals” (Roos, 1973) or “two apparent subunits which are 100 Å wide and separated by a 50–60 Å space” (Krishan, 1968; see also Brinkley and Stubblefield, 1966; Comings and Okada, 1971; Ris and Witt, 1981; Bernat et al., 1991). Indeed, although we now know that the vertebrate kinetochore outer plate is organized as a plate or “disk,” its tripartite nature led Brinkley and Stubblefield (1966, 1970)



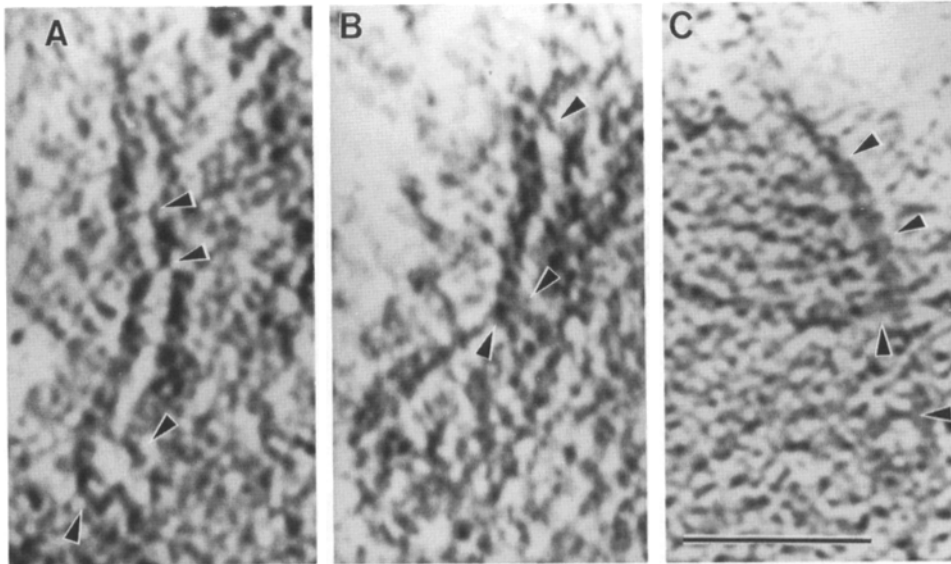


**Figure 5.** Examples of connection between the plate structure and the underlying chromatin as seen in 7.0-nm thick slices. Selected connecting fibers are indicated by arrowheads. The slices are from: (A) reconstruction 5; (B) reconstruction 6; and (C) reconstruction 1. Bar, 0.25  $\mu\text{m}$ .

to originally model this organelle as two “fibrils rather than tubules or laminated plates.”

Unfortunately, the tripartite nature of the outer plate has been largely overlooked in recent years as evidenced by the fact that it is not a feature of any contemporary models of kinetochore structure. Yet, considering the functional complexity of the outer plate, this feature may be important to kinetochore function. Many of the MTs which firmly connect each chromosome to the polar region and transmit the force for chromosome motion, terminate in the kinetochore outer plate (reviewed in Rieder, 1982, 1990; Brinkley et al., 1989). Tubulin microinjection studies reveal that these kinetochore MTs elongate and shorten, as the chromosome moves, by the addition and deletion of subunits at the kinetochore (Mitchison et al., 1986; Wise et al., 1991). Thus, the kinetochore is a complicated structure that is capable of holding its associated MTs while they switch between growing and shrinking states. Recent *in vitro* evidence also suggests that the kinetochore contains two separate MT-based molecular motors: one for moving the chromosome poleward (e.g., see Rieder and Alexander, 1990; Wordeman et al., 1991) and another for moving the chromosome away from the pole (Hyman and Mitchison, 1992). It is tempting to speculate that the separate structural domains inherent in a tripartite structure represent domains of separate function. For example, proteins associated with the fibers forming the outer domain could be responsible for holding the MTs, subunit exchange could occur within the middle translucent zone, and molecular “switches” controlling MT growth and shortening could be located in the domain closest to the chromo-

some. Moreover, although the motor for poleward motion is likely associated with the corona material extending from the plate (Rieder and Alexander, 1990; Wordeman et al., 1991), the molecules that allow newly incorporated MT segments to translocate poleward through the kinetochore, which is often coupled with movement away from the pole (see Mitchison, 1988, 1989; Wise et al., 1991), may be complexed to the holding site within the outer domain.

With the exception of the hypothesis proposed by Roos (1977), all contemporary models for kinetochore organization envision the outer plate to be connected to the subjacent chromosome by fibers entering and exiting the plate only at its peripheral edges (Ris and Witt, 1981; Rattner, 1986; Zinkowski et al., 1991). However, our data indicate that these connections are not restricted to the edges of the plate, but that they are distributed across its inner surface often in punctate linear arrays aligned perpendicular to the long axis of the chromosome (Figs. 5, A–C, 6 A and B, 9). This is consistent with the notion that the fibers that form the plate and connect it to the chromosome arise at multiple ordered points along the surface of the underlying (hetero) chromatin.

Zinkowski et al. (1991) recently proposed that the outer kinetochore plate is formed from “a continuous DNA fiber . . . that [is] folded and aligned into parallel register.” The parallel linear units formed by the looping fiber are envisioned to run perpendicular to the chromosome long axis, an arrangement that reflects the underlying organization of satellite DNA in the primary constriction. As might be predicted from such a model, we find that the outer plate is

**Figure 4.** Color-coded stereo volume renderings of windows from reconstructions 1 and 6. Different versions of reconstruction 1 were created by masking for distinct components of the kinetochore complex. The versions were coded and combined by placing each version in a different color channel of the computer graphics monitor. Each version was masked from a subvolume that included the major portion of the upper plate in Figs. 1 A and C, and 3. (A) An en face view of the plate structure from reconstruction 6 in the red channel (appears orange). (B) Same as A for reconstruction 1. (C) An edge view of the plate structure of reconstruction 1 in the red channel with the fibers that connect the plate to the chromosome in the green channel. Regions where the two versions overlap (i.e. where the connecting fibers are attached to the plate) are yellow. (D) The same as C except that the corona fibers are added to the blue channel. Regions where the corona fibers attach to the plate are purple while regions where corona and connecting fibers both attach are white. Bar, 0.25  $\mu\text{m}$ .

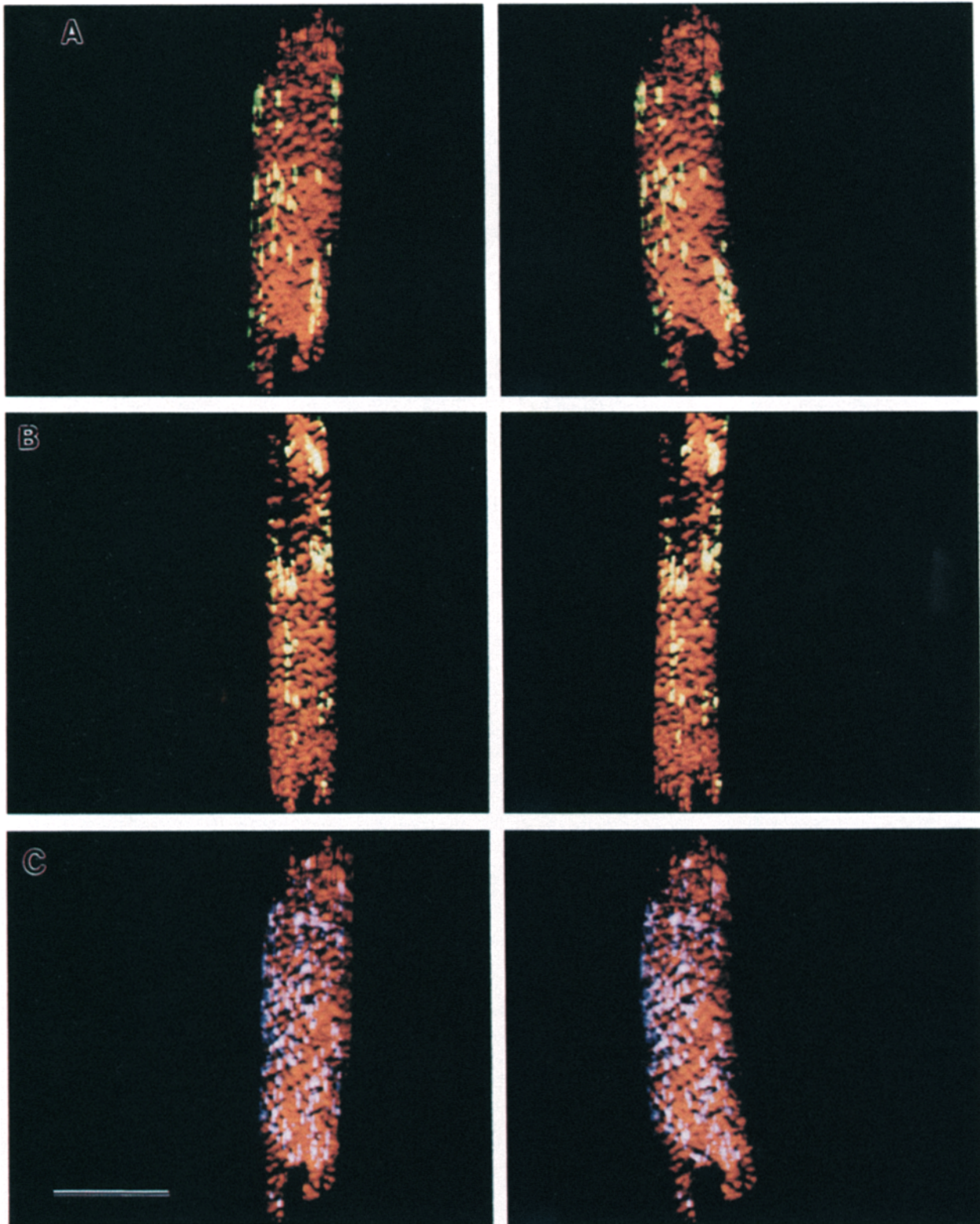


**Figure 6.** Location of attachment sites for connecting and corona fibers in stereo en face views of the plate. (A) Connecting fibers from reconstruction 1. Volume renderings of the plate are in the red channel, as in Fig. 4 B, with a double masked version of the reconstruction (see Materials and Methods) that isolates regions where the plate and connecting fibers overlap (i.e. where they are attached) in the green channel. (B) Connecting fibers viewed, as described in A, from reconstruction 3 (which is from a section sequential to reconstruction 1). (C) Corona fibers from reconstruction 1. The outer plate is in the red channel while the corona attachments are in the blue channel. Bar, 0.25  $\mu\text{m}$ .

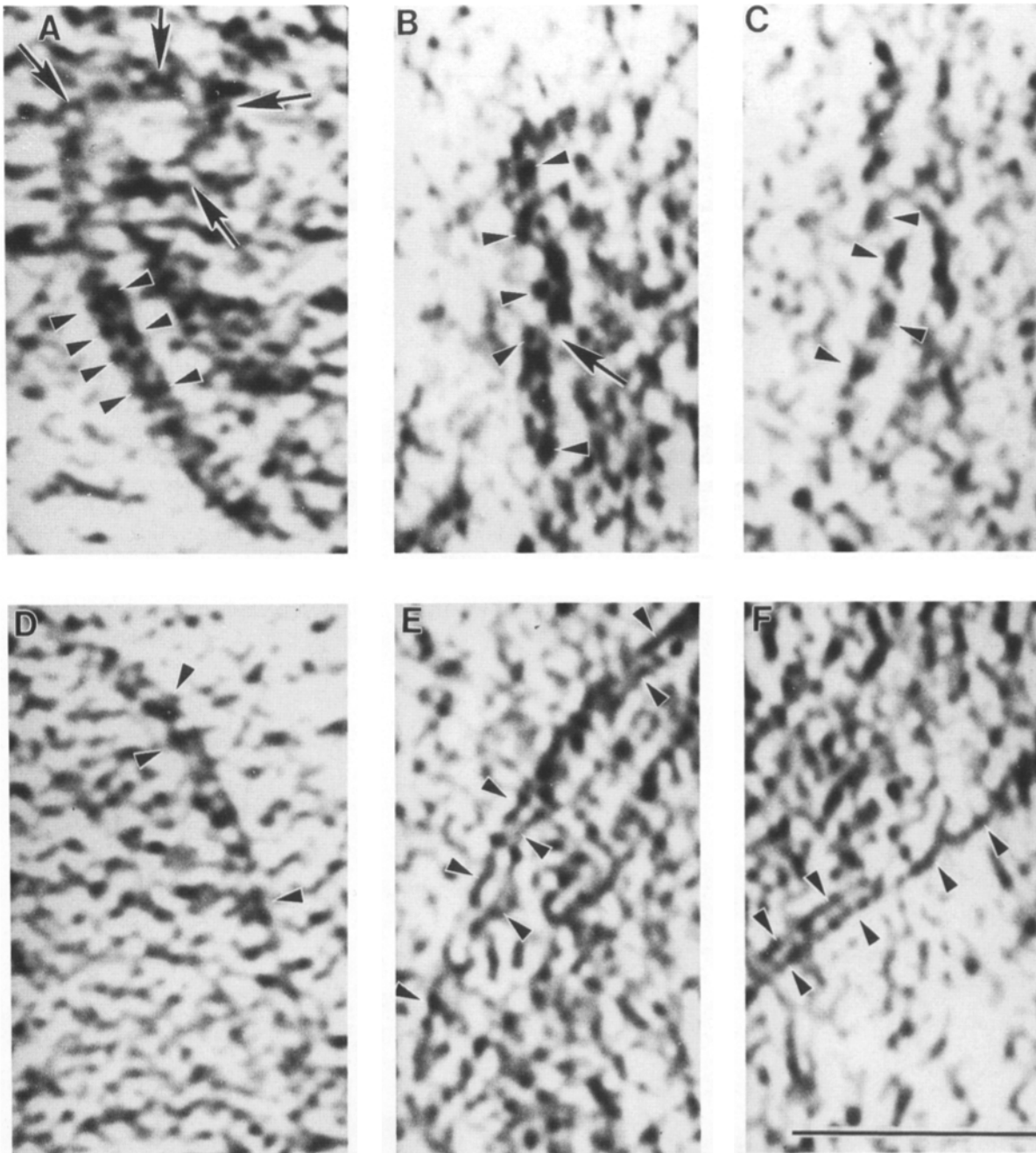


**Figure 7.** A representative set of kinetochore plate edge views seen in 7.0- or 10.5-nm thick slices. These views are taken from five different tomographic reconstructions. (*A* and *B*) Arrowheads denote a region where 10–20-nm electron opaque dots can be seen. Arrows mark a region of extreme curvature in *A* and an apparent discontinuity of the plate in *B*. (*C* and *D*) Arrowheads point to several 30–70-nm electron opaque beads or blocks. A tripartite composition is evident in *D*. (*E* and *F*) Arrowheads delineate parallel electron opaque fibers. Bar, 0.25  $\mu\text{m}$ .

attached to the underlying primary constriction by contacts arranged in linear arrays, perpendicular to the chromosome long axis (Figs. 6, *A* and *B*, 9). In addition, the plate often appears to be composed of multiple linear fibrils, 50–70 nm wide, that splay apart at its edges (e.g., Figs. 2 and 3). In accordance with this finding the plate, when viewed on edge and perpendicular to the chromosome long axis, often appears segmented into multiple unit blocks, each of which likely represents a close association of neighboring 10–20-nm thick fibers (Figs. 7, *C* and *D*, 8). Thus, although our

reconstructions clearly show that the fibers comprising the outer plate are not arranged in the orderly fashion predicted by Zinkowski et al. (1991), many of our findings are consistent with their hypothesis that the plate consists of “similar repetitive subunits”  $\sim 60$  nm in width.

As illustrated by the schematic diagram in Fig. 9, the structure of the kinetochore outer plate is not easy to comprehend. The difficulty arises from a curious mixture of order and randomness within its confines. On the one hand, the thickness of the plate is uniform (e.g., Figs. 1, 2), its

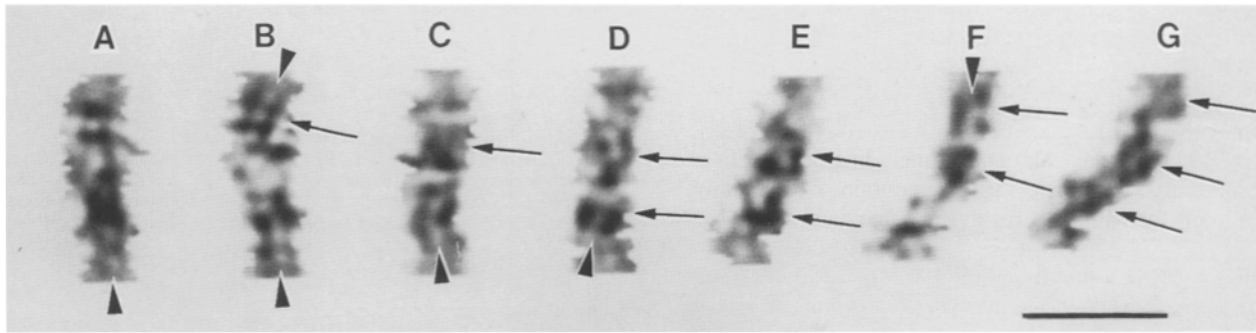


**Figure 8.** Selected 3.5-nm slices from a masked and windowed version of reconstruction 1. This is the same version as presented in Fig. 4 *B* but viewed here as thin slices from a direction that is edge on and perpendicular to the chromosomal long axis. Arrowheads indicate regions where the tripartite composition of the plate is visible whereas arrows denote 30-70-nm beads/blocks. Bar, 0.10  $\mu\text{m}$ .

boundaries on both the chromosome and cytoplasmic facing surfaces are distinct (e.g., Figs. 2, 5, 7, 8), and connections between the plate and chromosome are arranged in a somewhat orderly array (Fig. 6). Yet, despite local regions of parallel alignment and hints of a lattice structure, there is no readily discernible pattern to the overall arrangement of the 10-20-nm unit fibers (e.g., Figs. 4, *A* and *B*, 9). Spacing between fibers varies from where two or more fibers are fused together, to where there are remarkably wide gaps in the

plate structure (Figs. 4 *A*, 7, *B-D*, 8), with a similar degree of variation in the apparent fiber lengths observed in en face views (Fig. 4, *A* and *B*). Furthermore, the plate periphery is not tightly bound but tends to fray apart in the direction along the long axis of the chromosome. Finally, the third boundary of the structure (perpendicular to the chromosomal long axis but in the plane of the plate) is often indistinct making it difficult to determine exactly where the plate ends (e.g., Fig. 7 *D*). Thus, earlier models of the outer

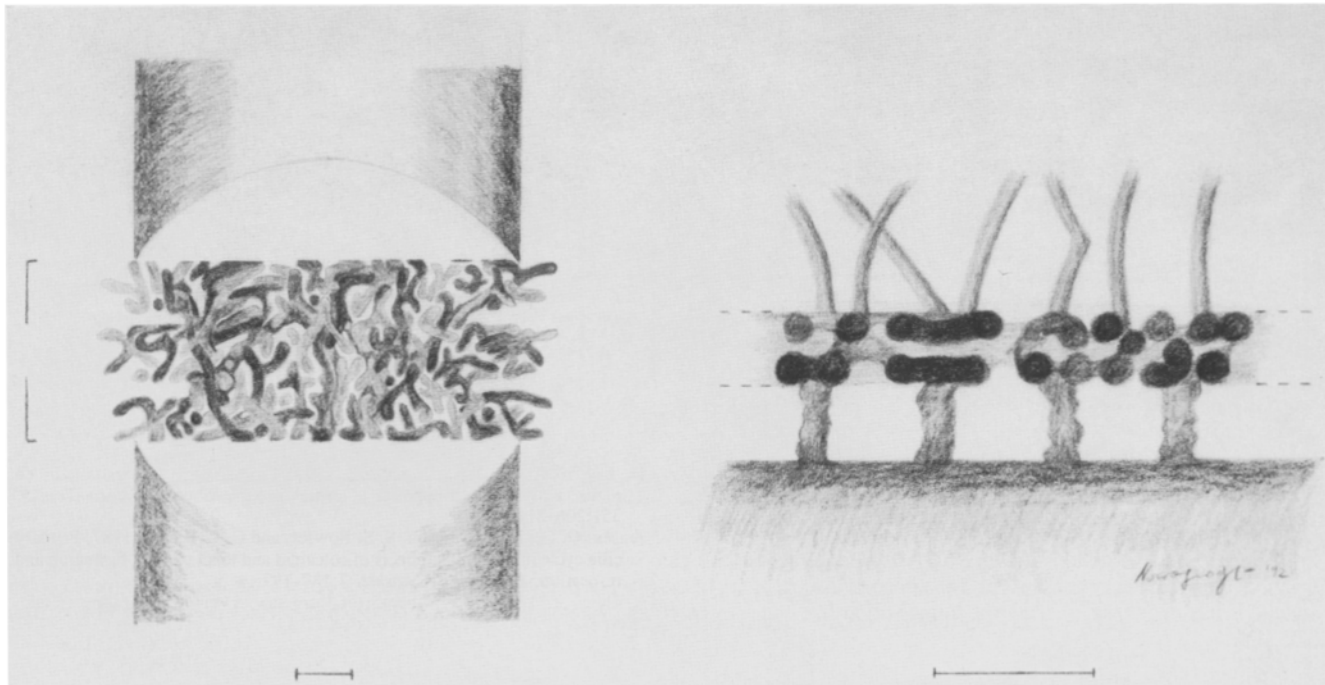


**Figure 9.** Schematic interpretation of the kinetochore outer plate structure as determined from our reconstructions. The illustrations depict the information in a single 185-nm thick section cut from the center of the kinetochore disk, perpendicular to the chromosomal long axis. (*Left*) En face view depicting a plausible arrangement of 10-20-nm thick unit fibers. Although there are small regions of parallel alignment and hints of a lattice, the fibers are generally variable in their orientation, apparent length, and spacing. In some regions two or three fibers form larger bundles whereas in other regions, large gaps are seen in the structure. The plate frays into three 60-nm wide "fingers" in a direction perpendicular to the chromosomal long axis. (*Right*) Edge view at higher magnification. In addition to the 10-20-nm fibers of the outer plate, the corona fibers and fibers connecting the plate to the underlying chromosome are also illustrated. The latter are spaced  $\sim 60$  nm along the long axis of the chromosome. Due to their variable orientation, fibers in the outer plate appear either as solid circles (when viewed head on) or as lines (when viewed from the side in some regions). In some regions, the fibers fuse into clusters whereas elsewhere there are apparent gaps in the structure. The space between fibers is not empty but filled with a lighter staining amorphous material presumed to be associated proteins. All bars, 0.10  $\mu\text{m}$ .

plate structure that postulated an ordered arrangement of fibers (Ris and Witt, 1981; Rattner, 1986; Zinkowski et al., 1991) are easier to comprehend but have proved to be an oversimplification.

A semi-ordered arrangement of unit structures is present in several other cellular components including 30-nm chromatin fibers and MTs. The former maintain a reasonably uniform diameter without a regular arrangement of nucleosome subunits (Woodcock et al., 1991, 1992), whereas the latter have a helical lattice but with discontinuities (McEwen and Edelstein, 1980) and the number of protofilaments can vary (Burton et al., 1975) even along a single MT (Chrétien et al., 1992). For chromatin fibers reduced order may be attributed to the variable length of linker DNA between nucleosomes (personal communication, C. L. Woodcock, University of Massachusetts), while in MTs it presumably arises because the interactions between protofilaments are much weaker than those along protofilaments. The kinetochore outer plate is analogous to the chromatin fiber because both exhibit one uniform dimension without a discernable pattern of subunit arrangement. However, the outer plate also resembles MTs in that there must be a relatively strong interaction in one direction to keep the plate thickness constant, with weaker interactions in the plane of the plate that allow for a semi-random arrangement of fibers and fragmentation of the structure. Finally, like chromatin fibers and MTs, the kinetochore outer plate is a flexible structure (e.g., Fig. 7 A) and it is possible that introducing a degree of randomness is a common way of achieving flexibility in biological structures.

As the kinetochore acquires MTs, poorly characterized structural changes occur in the outer plate: its diameter shrinks significantly and the corona disappears (reviewed in Rieder, 1982). Our current tomographic reconstructions provide important novel information regarding how the unattached kinetochore plate is organized at a resolution limit of  $\sim 12$  nm. Ongoing development of unlimited tilt stages (Barnard et al., 1992), image restoration techniques (Carazo, 1992), and volume visualization software (Frank and McEwen, 1992) promise to provide better resolution and enhance the effectiveness of the technique. In the future we intend to combine these more accurate approaches to data collection and processing with improved specimen preparation procedures (i.e., high pressure freezing followed by substitution) to obtain a more comprehensive picture of kinetochore structure and how it changes as it acquires its associated MTs.

We are grateful to Mr. Gerald Rupp, Mr. Yu Liu, and Ms. Leah McEwen for the excellent technical assistance during different parts of this study and Ms. Susan Nowogrodzki for the illustrations in Fig. 9 and editorial assistance with the manuscript.

Financial support was provided by National Institutes of Health grants GM 40165 (to J. Frank), GM 40198 (to C. L. Rieder), and by Biotechnological Resource grant RR 01219, awarded by the National Center for Research Resources, Department of Health and Human Services/Public Health Service, to support the Wadsworth Center's Biological Microscopy and Image Reconstruction Facility as a National Biotechnological Resource.

Received for publication 13 May 1992 and in revised form 6 October 1992.

## References

Barnard, D. P., J. N. Turner, J. Frank, and B. F. McEwen. 1992. A 360°

- single-axis tilt stage for the high-voltage electron microscope. *J. Microsc.* 167:39-48.
- Bernat, R. L., M. R. Delannoy, N. F. Rothfield, and W. C. Earnshaw. 1991. Disruption of centromere assembly during interphase inhibits kinetochore morphogenesis and function in mitosis. *Cell*. 66:1229-1238.
- Brinkley, B. R., and E. Stubblefield. 1966. The fine structure of the kinetochore of a mammalian cell in vitro. *Chromosoma*. 19:28-43.
- Brinkley, B. R., and E. Stubblefield. 1970. Ultrastructure and interaction of the kinetochore and centriole in mitosis and meiosis. *Adv. Cell Biol.* 1:119-185.
- Brinkley, B. R., S.-M. Cox, and D. A. Pepper. 1980. Structure of the mitotic apparatus and chromosome after hypotonic treatment of mammalian cells in vitro. *Cytogenet. Cell Genet.* 26:165-174.
- Brinkley, B. R., M. M. Valdivia, A. Tousson, and S. L. Brenner. 1984. Compound kinetochores of the Indian muntjac: evolution by linear fusion of unit kinetochores. *Chromosoma*. 91:1-11.
- Brinkley, B. R., M. M. Valdivia, A. Tousson, and R. D. Balczon. 1989. The kinetochore: structure and molecular organization. In *Mitosis: Molecules and Mechanisms*. J. S. Hyams and B. R. Brinkley, editors. Academic Press, New York. 77-118.
- Burton, P. R., R. E. Hinkley, and B. G. Pierson. 1975. Tannic acid-stained microtubules with 12, 13, and 15 protofilaments. *J. Cell Biol.* 65:227-233.
- Carazo, J. M. 1992. The fidelity of 3D reconstructions from incomplete data and the use of restoration methods. In *Electron Tomography*. J. Frank, editor. Plenum Publishing Corp., New York. 117-164.
- Chrétien, D., F. Metoz, F. Verde, E. Karsenti, and R. H. Wade. 1992. Lattice defects in microtubules: protofilament numbers vary within individual microtubules. *J. Cell Biol.* 117:1031-1040.
- Comings, D. E., and T. A. Okada. 1971. Fine structure of kinetochore in Indian muntjac. *Exp. Cell Res.* 67:97-110.
- Compton, D. A., T. J. Yen, and D. W. Cleveland. 1991. Identification of novel centromere/kinetochore-associated proteins using monoclonal antibodies generated against human mitotic chromosome scaffolds. *J. Cell Biol.* 112:1083-1097.
- Cooke, C. A., R. L. Bernat, and W. C. Earnshaw. 1990. CENP-B: A major human centromere protein located beneath the kinetochore. *J. Cell Biol.* 110:1475-1488.
- Crowther, R. A., D. J. DeRosier, and A. Klug. 1970. The reconstruction of a three-dimensional structure from projections and its application to electron microscopy. *Proc. Roy. Soc. Lond. A*. 317:319-340.
- Earnshaw, W. C., and J. E. Tomkell. 1992. Centromere and kinetochore structure. *Curr. Opin. Cell Biol.* 4:86-93.
- Frank, J. 1992. Introduction: principles of electron tomography. In *Electron Tomography*. J. Frank, editor. Plenum Publishing Corp., New York. 1-13.
- Frank, J., and B. F. McEwen. 1992. Electron tomography's remaining problems: how to fill the wedge in Fourier space and how to see what you've got in real space. *Proc. Annu. EMSA Meeting*. 50:1062-1063.
- Frank, J., and M. Radermacher. 1986. Three-dimensional reconstruction of non-periodic macromolecular assemblies from electron micrographs. In *Advanced Techniques in Biological Electron Microscopy III*. J. Koehler, editor. Springer-Verlag, Berlin. 1-72.
- Frank, J., B. Shimkin, and H. Dowse. 1981. SPIDER—a modular software system for electron image processing. *Ultramicroscopy*. 6:343-358.
- Frank, J., B. F. McEwen, M. Radermacher, J. N. Turner, and C. L. Rieder. 1987. Three-dimensional tomographic reconstruction in high voltage electron microscopy. *J. Electron Microsc. Technique*. 6:193-205.
- Gilbert, P. F. C. 1972. Iterative methods for the three-dimensional reconstruction of an object from projections. *J. Theoret. Biol.* 36:105-117.
- Gorbysky, G. J., P. J. Sammak, G. G. Borisy. 1987. Chromosomes move poleward in anaphase along stationary microtubules that coordinate disassembly from their kinetochore ends. *J. Cell Biol.* 104:9-18.
- Hyman, A. A., and T. J. Mitchison. 1991. Two different microtubule-based motor activities with opposite polarities in kinetochores. *Nature (Lond.)*. 351:206-211.
- Jensen, G. G., E. A. Davison, S. S. Bowser, and C. L. Rieder. 1987. Primary cilia cycle in PtK<sub>1</sub> cells: effects of colcemid and taxol on cilia formation and resorption. *Cell Motil. Cytoskel.* 7:187-197.
- Krishnan, A. 1968. Fine structure of the kinetochore in vinblastine sulfate-treated cells. *J. Ultrastruct. Res.* 23:134-143.
- Lawrence, M. C. 1992. Least-squares method of alignment using markers. In *Electron Tomography*. J. Frank, editor. Plenum Publishing Corp., New York. 197-204.
- Luther, P. K., M. C. Lawrence, and R. A. Crowther. 1988. A method for monitoring the collapse of plastic sections as a function of electron dose. *Ultramicroscopy*. 24:7-18.
- Masumoto, H., H. Masukata, Y. Murao, N. Nozaki, and T. Okazaki. 1989. A human centromere antigen (CENP-B) interacts with a short specific sequence in aliphoid DNA, a human centromeric satellite. *J. Cell Biol.* 109:1963-1973.
- McEwen, B. F. 1992. Three-dimensional reconstructions of organelles and cellular processes. In *Electron Tomography*. J. Frank, editor. Plenum Publishing Corp., New York. 281-311.
- McEwen, B. F., and S. J. Edelstein. 1980. Evidence for a mixed lattice in microtubules reassembled in vitro. *J. Mol. Biol.* 139:123-145.
- McEwen, B. F., M. Radermacher, C. L. Rieder, and J. Frank. 1986. Tomographic three-dimensional reconstruction of cilia ultrastructure from thick sections. *Proc. Natl. Acad. Sci. USA*. 83:9040-9044.

- McEwen, B. F., M. J. Song, and W. J. Landis. 1992. Quantitative determination of mineral distribution in different collagen zones of calcifying tendon using high voltage electron microscopic tomography. *J. Comput. Assisted Microsc.* 3:201-210.
- Mitchison, T., L. Evans, E. Schulze, and M. Kirschner. 1986. Sites of microtubule assembly and disassembly in the mitotic spindle. *Cell.* 45:515-527.
- Mitchison, T. J. 1988. Microtubule dynamics and kinetochore function in mitosis. *Annu. Rev. Cell Biol.* 4:527-549.
- Mitchison, T. J. 1989. Chromosome alignment at mitotic metaphase: balanced forces or smart kinetochores? In *Cell Movement*. Vol 2. Alan R. Liss, Inc., New York. 421-430.
- Moses, M. J., and S. J. Coonce. 1974. Electron microscopy of kinetochores in whole mount spreads of mitotic chromosomes from HeLa cells. *J. Exp. Zool.* 189:115-120.
- Nicklas, R. B. 1989. The motor for poleward chromosome movement in anaphase is in or near the kinetochore. *J. Cell Biol.* 109:2245-2255.
- Radermacher, M. 1992. Weighted back-projection methods. In *Electron Tomography*. J. Frank, editor. Plenum Publishing Corp., New York. 91-115.
- Rattner, J. B. 1986. The organization within the mammalian kinetochore. *Chromosoma.* 93:515-520.
- Rattner, J. B. 1987. The organization of the mammalian kinetochore: a scanning electron microscope study. *Chromosoma.* 95:175-181.
- Rieder, C. L. 1982. The formation, structure, and composition of the mammalian kinetochore and kinetochore fiber. *Int. Rev. Cytol.* 79:1-58.
- Rieder, C. L. 1990. Formation of the astral mitotic spindle: Ultrastructural basis for the centrosome-kinetochore interaction. *Electron Microsc. Rev.* 3:269-300.
- Rieder, C. L., G. Rupp, and S. S. Bowser. 1985. Electron microscopy of semi-thick sections: Advantages for biomedical research. *J. Electron Microsc. Technique.* 2:11-28.
- Rieder, C. L., and S. P. Alexander. 1990. Kinetochores are transported poleward along a single astral microtubule during chromosome attachment to the spindle in newt lung cells. *J. Cell Biol.* 110:81-95.
- Ris, H., and P. L. Witt. 1981. Structure of the mammalian kinetochore. *Chromosoma.* 82:153-170.
- Roos, U.-P. 1973. Light and electron microscopy of rat kangaroo cells in mitosis. II. Kinetochore structure and function. *Chromosoma.* 41:195-220.
- Roos, U.-P. 1977. The fibrillar organization of the kinetochore and the kinetochore region of mammalian chromosomes. *Cytobiologie.* 16:82-90.
- Schrader, F. 1953. *Mitosis, the Movements of Chromosomes in Cell Division*. L. C. Dunn, editor. Columbia University Press, New York. 170 pp.
- Turner, J. N., D. P. Barnard, G. Matuszek, and C. W. See. 1988. High-precision tilt stage for the high-voltage electron microscope. *Ultramicroscopy.* 26:337-344.
- Wise, D., L. Cassimeris, C. L. Rieder, P. Wadsworth, and E. D. Salmon. 1991. Chromosome fiber dynamics and congression oscillations in metaphase PtK<sub>2</sub> cells at 23°C. *Cell Motil. Cytoskel.* 18:1313-1342.
- Wordeman, L., E. R. Steuer, M. P. Sheetz, and T. J. Mitchison. 1991. Chemical subdomains within the kinetochore domain of isolated CHO mitotic chromosomes. *J. Cell Biol.* 114:285-294.
- Woodcock, C. L. 1992. The organization of chromosomes and chromatin. In *Electron Tomography*. J. Frank, editor. Plenum Publishing Corp., New York. 313-357.
- Woodcock, C. L., B. F. McEwen, and J. Frank. 1991. Ultrastructure of chromatin. II. Three-dimensional reconstruction of isolated fibers. *J. Cell Sci.* 99:107-114.
- Woodcock, C. L., R. A. Horowitz, and D. A. Agard. 1992. Three-dimensional organization of chromatin fibers in situ examined by EM tomography. *Proc. Ann. EMSA Meeting.* 50:498-499.
- Zinkowski, R. P., J. Meyne, and B. R. Brinkley. 1991. The centromere-kinetochore complex: a repeat subunit model. *J. Cell Biol.* 113:1091-1110.